International Journal of Thermal Sciences 48 (2009) 1302–1310

Contents lists available at ScienceDirect

International Journal of Thermal Sciences

www.elsevier.com/locate/ijts

Probabilistic modeling of transient heat transfer and assessment of thermal reliability of fibrous insulation under aerodynamic heating conditions

Shu-yuan Zhao *, Bo-ming Zhang, Shan-yi Du

Center for Composite Materials and Structure, Harbin Institute of Technology, Harbin 150080, China

ARTICLE INFO

Article history:
Received 10 June 2008
Received in revised form 8 November 2008
Accepted 8 November 2008
Available online 4 December 2008

Keywords:
Probabilistic
Heat transfer
Insulation
Thermal reliability

ABSTRACT

In present paper, the probabilistic thermal analysis of the fibrous insulation subjected to aerodynamic heating conditions was performed to account for the uncertainties such as material properties, loading conditions and geometrical variations. The statistical analysis of thermal response showed that the response temperature was significantly dependent on time and location. Large variations in the statistics parameters were observed at the location where temperature slip occurred for the first one minute of entry. To identify the dominant variables which most influence temperature response scatter, the correlation coefficients of various variables were computed. The results showed that the aerodynamic heating temperature and initial temperature had significant effects for the considered locations. However, the extinction coefficient, the specific heat of virgin material and the solid fraction ratio had non-negligible effect on the back side temperature scatter of fibrous insulation. Furthermore, the relationship between the probabilistic thermal reliability and thickness factor of safety was developed. Quantitative as well as qualitative information is provided in the present methodology, which is valuable to the thermal analysis, design and testing of fibrous materials.

1. Introduction

High-temperature fibrous insulation has been recognized as potential candidate materials for metallic thermal protection system because of its low density and excellent heat-insulation performance. Thermal analysis plays an important role in the design of fibrous insulation subjected to severe aerodynamic heating. Heat transfer through a fibrous insulation involves combined modes of heat transfer, which are mainly conduction and radiation. The coupled heat transfer mechanisms often make the analysis and the design of insulation quite difficult. Traditional thermal analyses have been conducted by solving the heat transfer equation under the assumption that all the parameters are deterministic. However, a number of uncertainties exist in the thermal analysis of fibrous insulation. Fibrous ceramic insulation is known to display a considerable amount of scatter due to the fabrication-related parameters, such as fiber diameter and porosity. Large uncertainty can exist in the obtained material properties due to insufficient knowledge of materials thermal behavior, inherent variability and possible human errors in testing [1,2]. There can also be high uncertainty in the prediction of aerodynamic heat flux, due to factors such as scatter in the reentry trajectory and highly complex phenomena that are difficult to analyze [3]. It is reported that the largest heating uncertainties for the first Orbiter flight can be up to 15–101% [4]. In some cases, especially in complex systems, the effect of uncertainties can be more significant. In the traditional design of fibrous insulations, high factors of safety (FOS) value are utilized to compensate for the large uncertainties in these data. It is thought that the component would be safer with additional margin or thickness. Undoubtedly, this practice often leads to an overly conservative design. However, even with this conservative design approach, the actual margin in the design, and the resultant design thermal reliability, have been difficult to establish. It is becoming evident that deterministic analysis is not sufficient for the design of fibrous insulation with complex heat transfer mechanism under severe aerodynamic heating condition. An improved design approach, which is a probabilistic approach, needs to be developed for evaluating uncertainty effects in heat transfer of fibrous insulation and for assessing thermal reliability.

Probabilistic modeling in composite materials can be implemented using either a statistical approach or a non-statistical approach. The statistical approach, e.g., the Monte Carlo method, employs repetitive iterations for which random values of uncertain parameters are generated according to assumed probability distributions to obtain a sufficiently large number of samples. There have been many published examples of application of the Monte Carlo technique to thermal analysis. Kamiński studied the probabilistic homogenization of the heat conduction problem in the two-component composite materials where the probabilistic mo-

* Corresponding author.
E-mail address: angel.zsy@126.com (S.-y. Zhao).

1290-0729/$ – see front matter
doi:10.1016/j.ijthermalsci.2008.11.004

Nomenclature

c	specific heat of insulation	$J\,kg^{-1}\,K^{-1}$	
c_a	specific heat of aluminum plate	$J\,kg^{-1}\,K^{-1}$	
D_f	diameter of fibers	m	
d_g	gas collision diameter	m	
f	solid fraction ratio		
G	incident radiation	$W\,m^{-2}$	
K	Boltzmann constant	$J\,K^{-1}$	
k_a	thermal conductivity of aluminum plate	$W\,m^{-1}\,K^{-1}$	
k_c	thermal conductivity of insulation due to conduction	$W\,m^{-1}\,K^{-1}$	
k_g	gas thermal conductivity	$W\,m^{-1}\,K^{-1}$	
k_g^*	gas thermal conductivity at an atmospheric pressure	$W\,m^{-1}\,K^{-1}$	
Kn	Knudsen number		
k_s^*	thermal conductivity of fiber parent material	$W\,m^{-1}\,K^{-1}$	
L	insulation thickness	m	
l	aluminum plate thickness	m	
n	number of data points		
P	pressure	Pa	
Pr	Prandtl number		
P_r	reliability		
q_r''	radiant heat flux	$W\,m^{-2}$	
r	correlation coefficient		
S	sample standard deviation		
t	time	s	
T	temperature	K	
$T_c(t)$	back side temperature of fibrous insulation	K	
$T_h(t)$	temperature profile of hot surface	K	
x	spatial coordinate through the insulation thickness	m	
x_i	ith random variable		
$\bar{y}$	sample mean value		
y_i	observed value of the sample		

Greek symbols

α	thermal accommodation coefficient	
β	extinction coefficient	m^{-1}
$\overline{\gamma}$	gas specific heat ratio	
δ	characteristic length for gas conduction	m
ε_1	emittance of the septum plate	
ε_2	emittance of the aluminum plate	
Ω	domain of integration	
λ	molecular mean free path	m
μ	mean value	
ρ	density of fibrous insulation	$kg\,m^{-3}$
ρ_a	density of aluminum plate	$kg\,m^{-3}$
σ	Stefan–Boltzmann constant	$W\,m^{-2}\,K^{-4}$
ω	albedo of scattering	

Subscripts

app	applied
g	gas
lim	limit
s	solid

ments of the effective conductivities were computed by the use of the Monte-Carlo simulation [5]. Nakamura et al. investigated the probabilistic temperature response of Piggyback Atmospheric Reentry Technology Testbed using the Monte Carlo technique. The thermal conductivity of the macelite insulator, the emissivity of the C/C shell heat shield and aerodynamic heat flux were considered as random parameters [6]. Another example were found in simulating the thermal response of decomposing/ablating materials to predict insulation performance and to assess the reliability of a solid propellant rocket motor's internal insulation design [7]. An alternative way to perform the probabilistic thermal analysis is to use the non-statistical approach. Xiu presented a generalized polynomial chaos algorithm for the solution of transient heat conduction subjected to uncertain inputs: random thermal conductivity and specific heat [8]. Kamiński et al. presented the stochastic finite element analysis of transient heat transfer in a three-component layered composite with randomly defined thermal properties, based on the second order perturbation second central probabilistic moment method [9]. Nicolai et al. proposed a probabilistic finite element perturbation method for heat transfer problems with random variable thermophysical properties [10].

Current research effort is primarily directed towards the probabilistic thermal analysis and thermal reliability assessment of the fibrous insulation subjected to service conditions. A probabilistic behavior of the transient temperature response is performed to account for the uncertainties such as material properties, loading conditions and geometrical variations. To identify the dominant variables which most influence temperature response, the correlation coefficients of various variables are computed. Furthermore, the relationship between the probabilistic thermal reliability and insulation thickness FOS is developed.

2. Thermal response model description

A simplified thermal problem simulating re-entry aerodynamic heating conditions will be used in the present study. Schematic of thermal analysis model is shown in Fig. 1. An insulation sample is located between a septum plate and an aluminum plate. The septum plate is subjected to the transient radiation-equilibrium temperature distribution. The aluminum plate is assumed to be adiabatic. This is the standard assumption used for insulation design for space transportation vehicles, even though it has been shown to be very conservative.

Neglecting the effect of natural convective heat transfer within fibrous insulation, the conservation of energy can be written as [11]

$$\rho c\frac{\partial T}{\partial t}=\frac{\partial}{\partial x}\left(k_c\frac{\partial T}{\partial x}\right)-\frac{\partial q_r''}{\partial x} \tag{1}$$

in fibrous insulation and

$$\rho_a c_a\frac{\partial T}{\partial t}=\frac{\partial}{\partial x}\left(k_a\frac{\partial T}{\partial x}\right) \tag{2}$$

in the aluminum plate.

Subject to the following initial and boundary condition:

$$T(x,0)=T_0 \tag{3}$$

$$T(0,t)=T_h(t) \tag{4}$$

$$\left.\frac{\partial T}{\partial x}\right|_{x=L+l}=0 \tag{5}$$

At the interface between the aluminum plate and the fibrous insulation, energy conservation leads to

$$\left(k_c\frac{\partial T}{\partial x}-q_r''\right)_{x=L-}=\left(k_a\frac{\partial T}{\partial x}\right)_{x=L+} \tag{6}$$

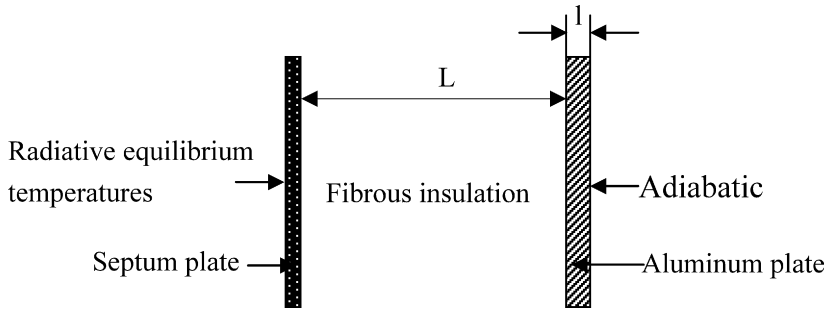

Fig. 1. Schematic of thermal analysis model.

For simplicity, no contact resistance is assumed to exist at the interface between the insulation and the aluminum plate.

The gradient of the radiant heat flux is given by [12]

$$\frac{\partial q_r''}{\partial x} = \beta(1-\omega)(4\pi I_b - G) \tag{7}$$

Although a more accurate model as developed by Yuen [13] can be used to evaluate the radiation heat transfer through fibrous insulation, the two-flux approximation is used for the current analysis in order to save the computational cost. This method has been used by Daryabeigi [14] and Marschall [15] to calculate the radiation heat transfer within fibrous insulation under aerodynamic heating conditions. The radiant heat flux in fibrous insulation is related to incident radiation, G, according to:

$$q_r'' = -\frac{1}{3\beta}\frac{\partial G}{\partial x} \tag{8}$$

The second order differential equation governing the incident radiation are solved subject to the following boundary conditions

$$q_r''(0,t) = \frac{\varepsilon_1}{2(2-\varepsilon_1)}\left[4\pi I_b\left(T_h(t)\right) - G(0,t)\right] \tag{9a}$$

$$q_r''(L,t) = \frac{\varepsilon_2}{2(2-\varepsilon_2)}\left[4\pi I_b\left(T_c(t)\right) - G(L,t)\right] \tag{9b}$$

In the present study, it is assumed that $\varepsilon_1 = 0.8$ and $\varepsilon_2 = 0.3$.

The combined thermal conductivity due to solid conduction and gas conduction in fibrous insulation is given by [16]

$$k_c = f^2 k_s^* + \frac{k_g - f^2 k_s^*}{1 + \frac{f}{1-f}\left[1 + \frac{5}{6}\frac{k_g - f^2 k_s^*}{k_g + f^2 k_s^*}\right]} \tag{10}$$

The effect of pressure on the thermal conductivity of a gas can be investigated by the way of the Maxwell moment method [17,18] and temperature jump theory [19]. Daryabeigi used temperature jump theory to model the gas conduction in fibrous insulation, and the gas thermal conductivity is described as [20]

$$k_g = \frac{k_g^*}{\phi + \psi \cdot 2\frac{2-\alpha}{\alpha}\left(\frac{2\bar{\gamma}}{\bar{\gamma}+1}\right)\frac{1}{Pr}Kn} \tag{11}$$

The parameters ϕ and ψ depend on the Knudsen number. $\phi = 1$, $\psi = 0$ for Knudsen number less than 0.01 (continuum regime), $\phi = 1$, $\psi = 1$ for Knudsen number between 0.01 and 10 (transition regime), and $\phi = 0$, $\psi = 1$ for Knudsen number greater than 10 (free-molecular regime). The Knudsen number, Kn, is calculated from

$$Kn = \frac{\lambda}{\delta} \tag{12}$$

λ is given by

$$\lambda = \frac{KT}{\sqrt{2}\pi d_g^2 P} \tag{13}$$

and δ is given by

$$\delta = \frac{\pi}{4}\frac{D_f}{f} \tag{14}$$

The solution to the governing conservation of energy equation can be obtained using an iterative procedure. The distribution of incident radiation is obtained in the region by solving Eq. (7) combined Eq. (8) subject to the boundary conditions in Eqs. (9a) and (9b), and the radiant flux is obtained according to Eq. (8). The gradient of radiant heat flux is obtained using Eq. (7), and substituted in the energy equation to solve for the temperature distribution in the domain. More detailed descriptions about the solution of the heat transfer model are provided in Ref. [21].

3. Model validation

For validation purpose, the numerical model was utilized to perform thermal analysis of a test assembly, and then the predicted results were compared with experimental results in Ref. [14]. As described in detail in Ref. [14], the test article, a 53.3 mm thick fibrous insulation sample with a density of 45.1 kg/m^3, was placed between the Inconel and aluminum panels. The Inconel panel served as the hot side solid boundary, while the aluminum panel represented the launch vehicles structure. A 13.3 mm thick aluminum fibrous insulation with a density of 24.3 kg/m^3 was placed between the aluminum panel and the water-cooled plate. The measured transient temperatures of the septum panel and water-cooled plate from Fig. 2a were used as boundary conditions in the numerical model, and the measured temporal variations of the chamber pressure from Fig. 2b were used for gas conduction calculations. The predicted temperatures of the aluminum panel located between fibrous insulation samples with thicknesses of 53.3 and 13.3 mm in present study were compared with the experimental data, and the result is shown in Fig. 3. The maximum difference between the numerically predicted and ground-test measured aluminum panel temperatures was 13.8 K. The maximum relative difference was 2.9%. The close agreement between measured and predicted aluminum panel temperatures validated the numerical model for predicting the transient thermal performance of the fibrous insulation subject to reentry aerodynamic heating conditions.

4. Probabilistic analysis technique

The primary function of fibrous insulation is to restrict heat flow and maintain the underlying structures within acceptable temperature limit during re-entry aerodynamic heating. Little overtemperature may lead to catastrophic effects. Therefore, the temperature response at any point at any time during the entry exceeding the maximum allowable bondline temperature can be considered as a failure. Following this failure criteria, the margin of safety for a fibrous insulation is defined as

$$g(x) = T_{\lim} - T_{\text{app}}(x_1, x_2, \ldots, x_n) \tag{15}$$

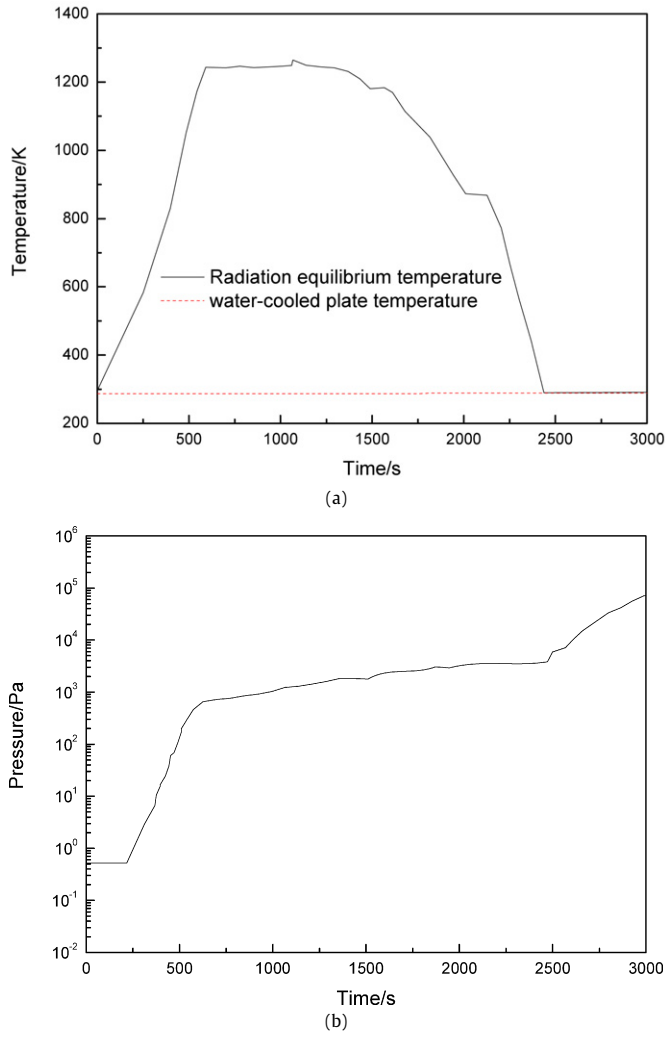

Fig. 2. Ground-test measured radiation equilibrium temperature and water-cooled plate temperature profile (a) and pressure history (b) in Ref. [13].

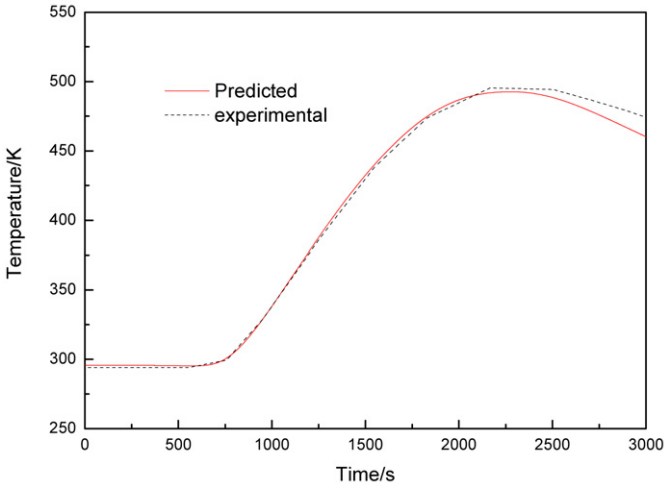

Fig. 3. Comparison of predicted results in present study with the experimental data [13].

$g(x)$, which is also called a limit state function, can be an implicit or explicit function of random variables and is divided in such a way that $g(x) = 0$ is a boundary between the failure region $g(x) < 0$ and safe region $g(x) > 0$. Given the probability density

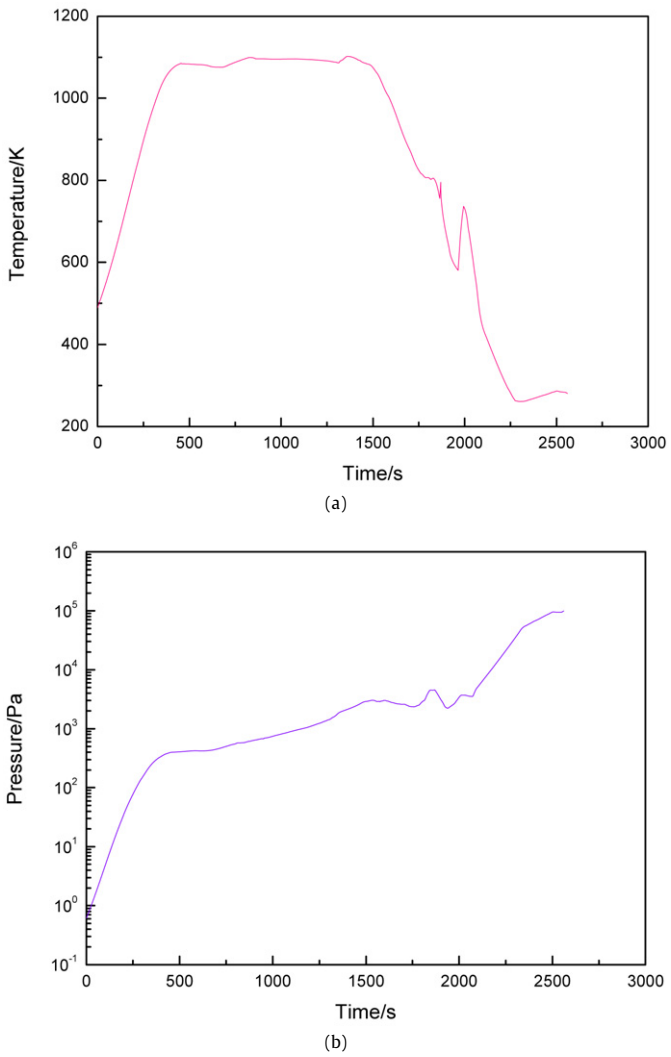

Fig. 4. Typical radiation equilibrium temperature (a) and pressure (b) profile for RLV entry.

function $f_x(x)$ of the limit state function $g(x)$, we can formulate the reliability P_r as

$$P_r = P\left[g(x) > 0\right] = \int_{\Omega} \cdots \int f_x(x)\, dx \tag{16}$$

This multiple integration is, in general, very difficult to evaluate analytically.

In the present study, Monte Carlo method is employed to evaluate uncertainty effects and assess thermal reliability, as it is flexible, easy and efficient for very complicated physical even coupled models, just like the thermal analysis of fibrous insulation with complex heat transfer mechanisms under aerodynamic heating condition. Alumina fibrous insulation with a density of 48.6 kg/m^3 is investigated. The sample thickness used in this analysis is 74.064 mm. This is the minimum thickness of fibrous insulation determined from the deterministic analysis for the nominal loading environment relative to the maximum allowable temperature limit, which is also called the "zero-margin thickness".

As discussed above, a number of uncertain parameters are incorporated in thermal analysis of fibrous insulation subjected to aerodynamic heating. These parameters can affect the temperature response and therefore can be included as random variables. The current probabilistic analysis selects a total of eight parameters: four are thermal property parameters, three are load parameters,

Table 1
Definitions of random variables.

Variable	Mean value
Radiation equilibrium temperature (K)	$T_h(t)$
Pressure (Pa)	$P(t)$
Initial temperature (K)	$T_0 = 290$
Thermal conductivity of virgin material (W/(m K))	$k_s^* = 12082.81/T - 4.191$
Specific heat of virgin material (J/(kg K))	$c = -0.3 + 3.589T - 3.686 \times 10^{-3}T^2 + 1.315 \times 10^{-6}T^3$
Solid fraction ratio	$f = 0.0147$
Extinction coefficient (1/m)	$\beta = 2037.312 + 0.91368T$
Mean fiber diameter (μm)	$D_f = 3$

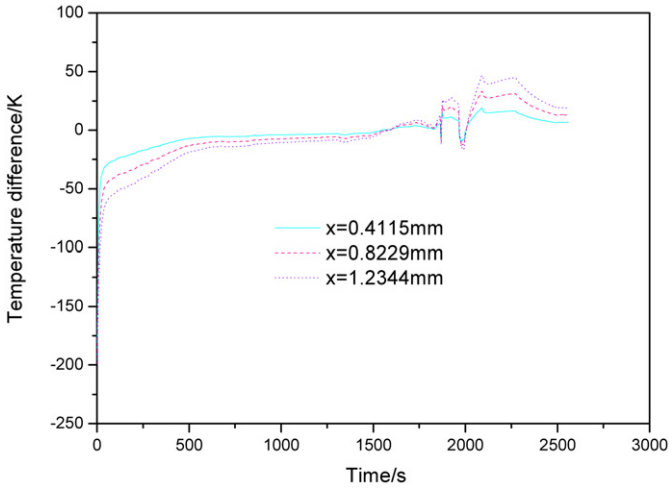

Fig. 5. Temperature slip behavior near the heating surface.

and one is geometrical parameter. To facilitate the analysis, all the random variables are assumed to be independent and normal distribution. A scatter of ±5% is specified for all the variables. The definitions of the random parameters are shown in Table 1. Typical radiation equilibrium temperature and surface pressure profiles for Reusable Launch Vehicle (RLV) entry are shown in Fig. 4 [22]. The maximum allowable temperature (421.9 K for the current analysis [22]) is also assumed to be normal distribution with the coefficient of variation (COV) of 5%. Although the distributions and variations of random parameters chosen may not be realistic, any other statistical distributions with different variations can be easily realized in this probabilistic thermal analysis framework.

In the current study the probabilistic thermal analysis is implemented as illustrated in the following procedure:

(1) The input random variables are identified, and the corresponding probabilistic distributions are selected. For a given set of random variables, a deterministic thermal analysis is run using a finite difference technique. The response results are collected from the thermal analysis output.
(2) The whole process is repeated a number of times to generate a table of response variable values that correspond to the perturbed values of the selected input random variables.
(3) The probabilistic thermal analysis then uses the previously generated table to compute the statistical characteristics of the thermal response, correlation coefficient of input–output and thermal reliability.

5. Results and discussion

Due to the high porosity of the material and high scattering coefficient, a temperature change which is larger than 100 K can occur over a distance of less than 2 mm, as shown in Fig. 5. Therefore, two locations, $x = 0.823$ mm (designated as A) where temperature slip occurs and $x = 74.064$ mm (designated as B) which is the back surface of the fibrous insulation, are selected to investigate the statistical characteristics of thermal response and correlation of input–output parameters for the current analysis.

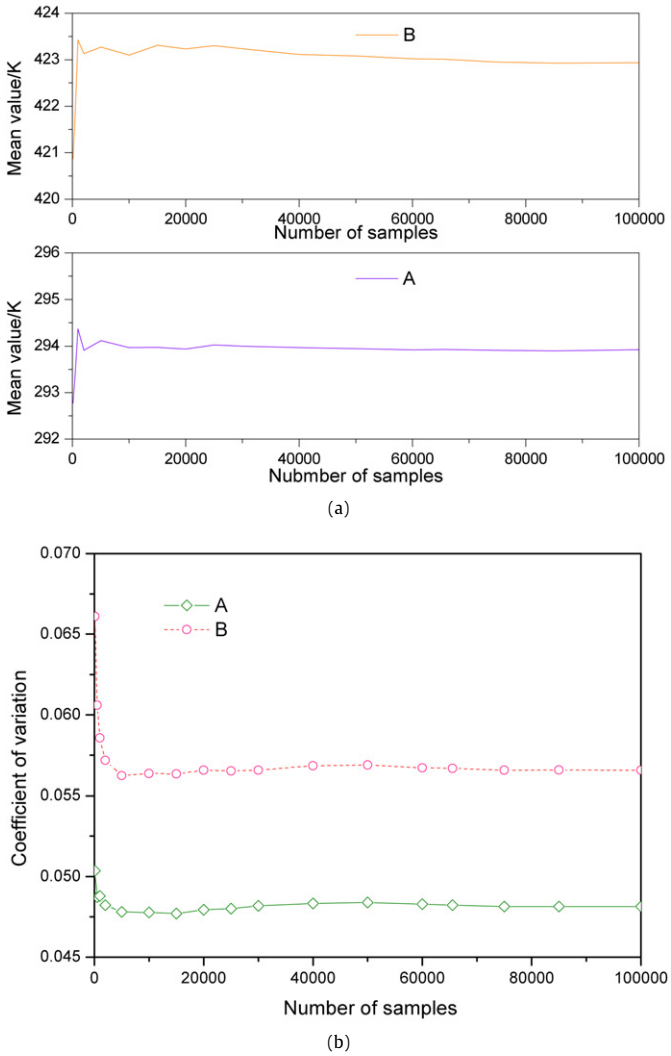

Fig. 6. The impact of the number of samples on mean values (a) and coefficient of variation (b).

The impact of the number of Monte Carlo samples on the accuracy of the model result is investigated. The mean values and coefficient of variations as a function of the number of Monte Carlo samples are shown in Fig. 6. From the figures, it can be seen that 20000 samples appear to be a good compromise between accuracy and numerical cost. For this reason, the probabilistic transient thermal response and correlation of input–output parameters are analyzed using 20000 Monte Carlo samples. However, 100 000

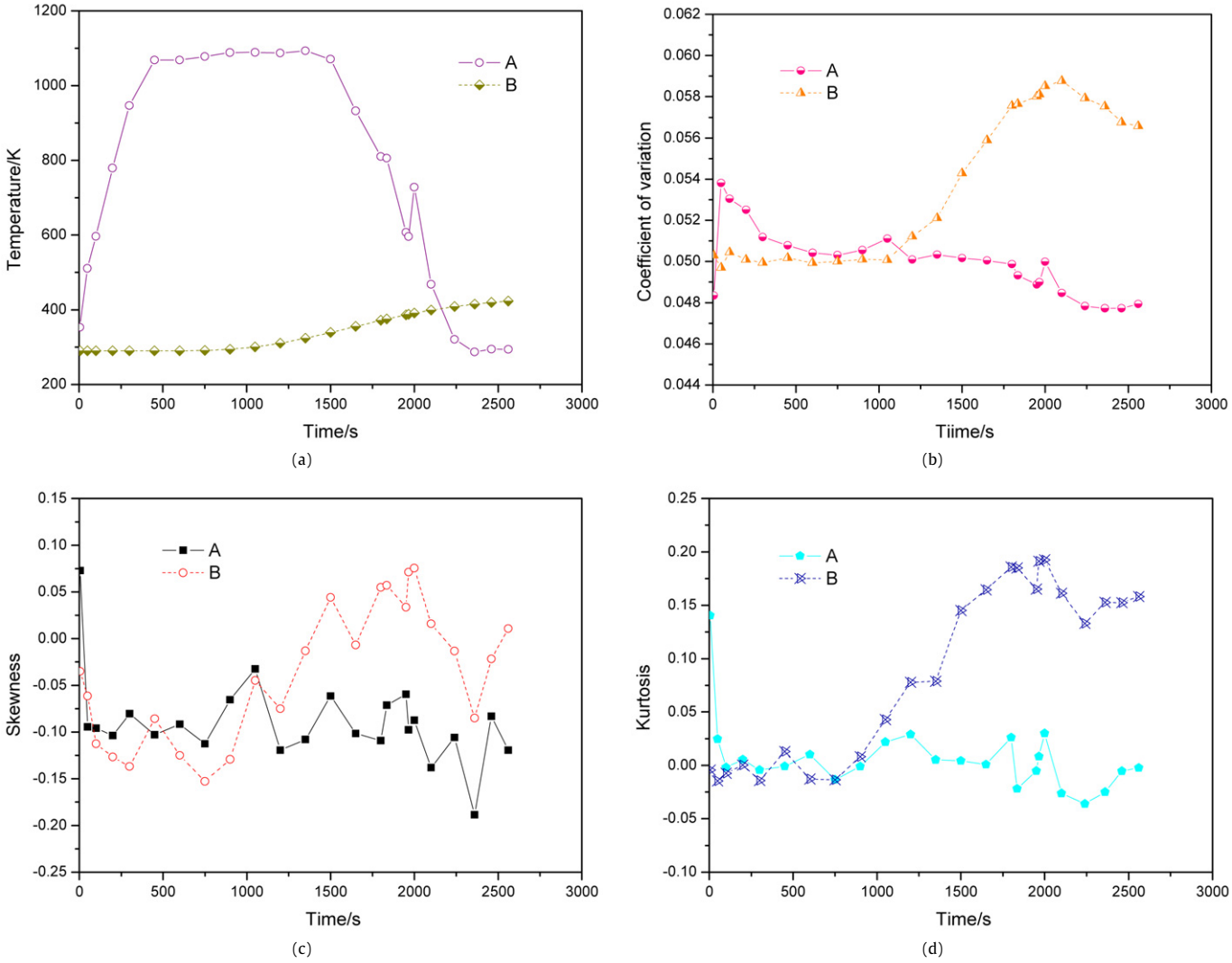

Fig. 7. Statistical characteristics of temperature responses at A and B (a) mean value; (b) coefficient of variation; (c) skewness; (d) kurtosis.

samples are used to calculate the index of reliability and thermal reliability of fibrous insulation.

5.1. Statistical characteristics of probabilistic transient thermal response

A statistical analysis for the probabilistic thermal responses at locations A and B is performed. This analysis includes the mean value, coefficients of variation, skewness and kurtosis of thermal responses. The coefficient of variation, skewness and kurtosis are defined by:

$$\mathrm{COV} = \frac{S}{\bar{y}} \tag{17}$$

$$\mathrm{Skewness} = \frac{n}{(n-1)(n-2)} \sum_{i=1}^{n} \left(\frac{y_i - \bar{y}}{S} \right)^3 \tag{18}$$

$$\mathrm{Kurtosis} = \left[\frac{n(n+1)}{(n-1)(n-2)(n-3)} \sum_{i=1}^{n} \left(\frac{y_i - \bar{y}}{S} \right)^4 \right] - \frac{3(n-1)^2}{(n-2)(n-3)} \tag{19}$$

The mean value, coefficient of variation, skewness and kurtosis of thermal response at the selected two locations are shown in Figs. 7a–7d. Obviously, these statistical parameters are time-dependent. The mean value of the back side temperature of fibrous insulation increases with the reentry time period. From Fig. 7b, we can see that the COV at A increases sharply for the first one minute of entry and then decreases to around 5%. The COV of thermal response at B initially increases with the time period and reaches a peak at around 2100 seconds, and then decreases somewhat. It is found in Fig. 4b that the COV at each location reaches its peak before the mean temperature attains the peak value. This is in accordance with the results obtained by Xiu et al. [8] and Nakamura et al. [6]. It is also noticed that the maximum COV of output parameters can be up to 6% though the COV of all the input random parameters is 5%, which indicates that the uncertainty effect can be enlarged. Skewness is a measure of symmetry. Negative values for the skewness indicate data that are skewed left and positive values for the skewness indicate data that are skewed right. Kurtosis is a measure of whether the data are peaked or flat relative to a normal distribution. In Figs. 7c and 7d, it is interesting to note that the skewness and kurtosis at the location A decrease rapidly within one minute of entry, contrasting with the sharp increase in the COV. Then negative values for the skewness are observed at A and the kurtosis fluctuates around zero after that time period. However, whether the temperature data at B are skewed left or right is time-dependent. The kurtosis of temperature response data at this location becomes positive after some time periods, which means that the temperature response appears to be peaked relative to a normal distribution. The probability density functions of

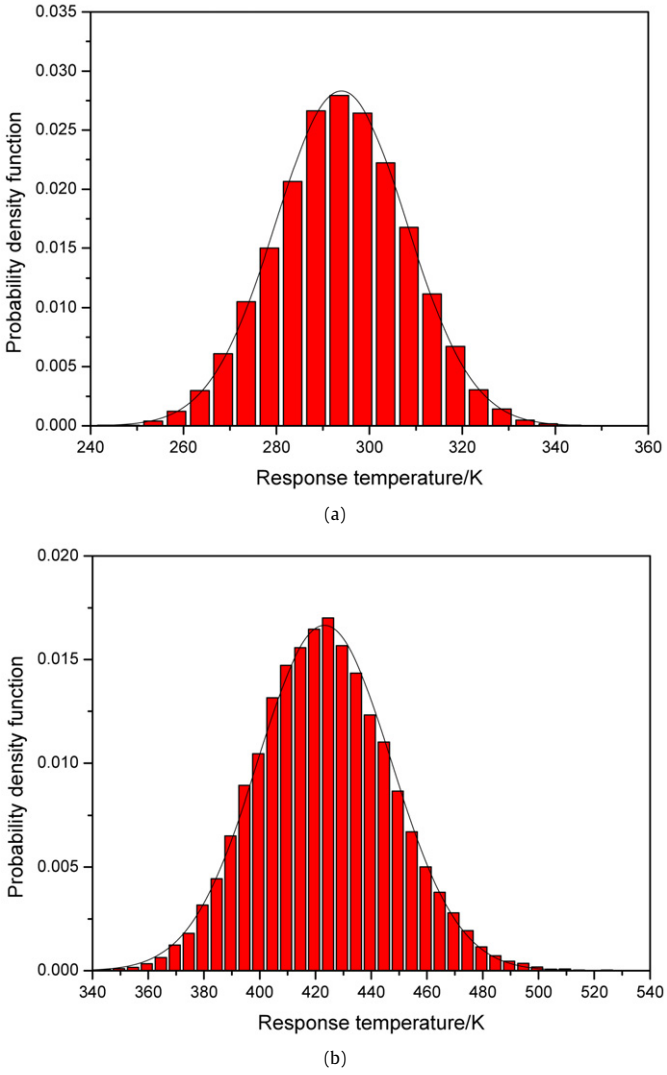

Fig. 8. Probability density functions of response temperatures at different locations at the end of reentry (a) location A; (b) location B.

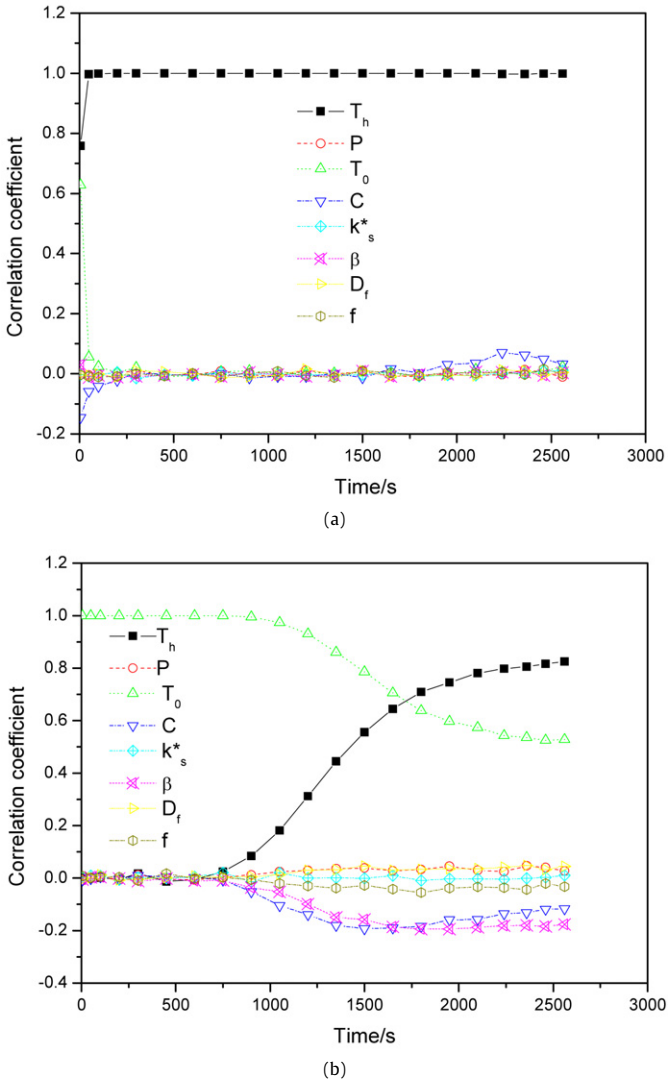

Fig. 9. Correlation coefficients at different locations (a) location A; (b) location B.

response temperatures at A and B at the end of reentry are shown in Fig. 8.

5.2. Correlation analysis of input–output parameters

Note that, for a nonlinear system, it is generally not possible to rigorously separate the contributions of each input parameter to the output uncertainty. Nevertheless, a linear regression analysis is often employed to roughly gauge the uncertainty contributions. The correlation coefficient is given by

$$r = \frac{\sum_{i=1}^{n}(x_i - \bar{x})(y_i - \bar{y})}{\sqrt{\sum_{i=1}^{n}(x_i - \bar{x})^2}\sqrt{\sum_{i=1}^{n}(y_i - \bar{y})^2}} \tag{20}$$

The correlation coefficient can be interpreted as the fractional contribution to the uncertainty in the output due to uncertainty in a given input parameter. The magnitude of the correlation coefficient provides a way to rank the importance of the individual physical variables. If the absolute value of correlation coefficient is close to unity, the parameter strongly affects the temperature response at that location. On the other hand, if the correlation coefficient is close to zero, the parameter has little contribution to the temperature response. Evaluating the correlation coefficients can therefore offer good insight into the mechanism of the temperature response.

The correlation coefficients between the random input parameters and the temperature responses are calculated at different time periods, and the results are shown in Fig. 9. Fig. 9a indicates that the radiative equilibrium temperature, initial temperature and specific heat of virgin material have significant effect on the temperature response at A for the first one minute of entry. The radiative equilibrium temperature remains to be the most important parameter affecting the response temperature from beginning to end. This is because the aerodynamic heating temperature is the main source of heat to fibrous insulation at the location near the heating surface. It can be stated that the correlation coefficient of the specific heat of virgin material changes sign from negative to positive, indicating that the response temperature at A firstly decreases and then increases with the increase of the specific heat of virgin material. From Fig. 9b, the initial temperature has significant effect on the response scatter at B at the beginning, and then the radiative equilibrium temperature becomes more and more important with the increase of duration. The temperature response at this location increases with the increase of the initial temperature and the hot side temperature. Therefore, a characterization or control of the load environment improves, and COV approaches zero, the reliability increases. It is pointed out that the extinction coeffi-

cient, the specific heat of virgin and the solid fraction ratio, which shows negative correlations, have non-negligible effect on the response scatter at B. The correlation coefficient of the specific heat of virgin material to the temperature is negative at B, contrary with positive at A at the end of time. It is indicated that if we were to experimentally determine the properties of such a composite material, we could expect values anywhere in the range indicated by the scatter. Such information obviously gives a test engineer useful insight with which to design and plan the test setup and the number of tests for a particular material study.

The response scatters at both locations seem to be unaffected by aerodynamic pressure, fiber mean diameter and the solid thermal conductivity. This is attributed to the fact that the radiative contribution dominates the heat transfer in reentry conditions (i.e. high temperature and vacuum pressures) [23,21]. However, these parameters are related with conduction heat transfer, solid or gas. Therefore, such parameters can be considered as deterministic variables in the fibrous insulation thermal analysis under aerodynamic heating condition.

5.3. Factor of safety and thermal reliability

In developing components or systems to satisfy a reliability requirement, it is necessary to design for the nominal environment, and also evaluate the capability to withstand occasional, off-nominal events. Following conventional machine design formalism, methodology was developed to assess the factors of safety and thermal reliability for thermal protection system in Ref. [24]. Thermal load, temperature and thickness can be considered as assessing variables. The index of reliability provides a probabilistic estimated reliability for the nominal environment. Using the temperature variables, the index of reliability (IOR) of fibrous insulation is given by

$$\mathrm{IOR} = \frac{\mu_{\mathrm{lim}} - \mu_{\mathrm{app}}}{\sqrt{S_{\mathrm{app}}^2 + S_{\mathrm{lim}}^2}} \tag{21}$$

The thermal reliability of the fibrous insulation can be estimated by analysis of the interference between the strength and load distributions [25]. For normal probability distributions of strength and load, thermal reliability is defined by:

$$P_r = \frac{1}{\sqrt{2\pi}} \int_{-\infty}^{\mathrm{IOR}} \exp\left(-\frac{x^2}{2}\right) dx \tag{22}$$

Reliability increases with increasing the FOS. In other words, increasing the FOS, for example, by increasing the insulation thickness provides additional insulation of the structure and improves its thermal reliability. The variation of the IOR with the thickness FOS value for insulation is shown in Fig. 10. The thickness FOS value is the ratio of the applied and the limit thickness. The thermal reliability of fibrous insulation can be obtained either by the approach as mentioned above or by the standard Monte-Carlo simulation technique. The thermal reliability versus the thickness FOS value using the two methods is shown in Table 2. The results show that agreement between the two is excellent. The reliability increases rapidly from 49 to 97% when the thickness FOS value increases from 1 to 1.3, and then increases very slowly for the investigated range. In order to yield an IOR value of 3, a resulting reliability of 99.9%, the thickness FOS value should be larger than 1.5 for the current investigated uncertainty conditions. The IOR can be up to 4.74 when the thickness FOS value is 2. These results provide quantitative as well as qualitative information that can be used in the optimal design of thermal insulation materials.

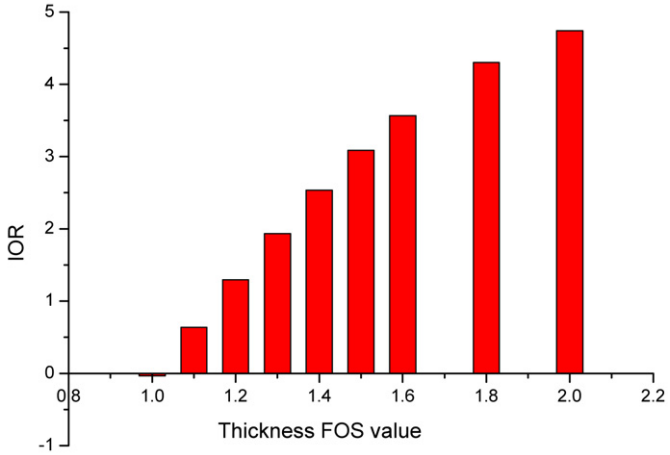

Fig. 10. Variation of index of reliability with thickness FOS value.

Table 2
The predicted thermal reliability versus thickness FOS value.

Thickness FOS value	Thermal reliability	
	Load interference	Monte Carlo (mean + 95% confidence level)
1	0.48685	0.49126 ± 0.00260
1.1	0.73800	0.74248 ± 0.00228
1.2	0.90269	0.90243 ± 0.00154
1.3	0.97349	0.97180 ± 0.00086
1.4	0.99439	0.99423 ± 0.00039
1.5	0.99898	0.99872 ± 0.00019
1.6	0.99982	0.99963 ± 0.00010
1.8	0.99999	0.99993 ± 0.00004

6. Conclusion

In the present work, the probabilistic thermal analysis of the fibrous insulation subjected to service conditions was performed using Monte Carlo technique, taking into account the scatter in material properties, loading conditions and geometrical variations. The statistical analysis of thermal response showed that the response temperature was significantly dependent on time and location. Large variations in statistical parameters were observed at the location where temperature slip occurred for the first one minute of entry. Evaluation of the contributions of the random parameters to the temperature response showed that the aerodynamic heating temperature and initial temperature had significant effects for the considered locations. However, extinction coefficient, the specific heat of virgin and the solid fraction ratio had non-negligible effect on the back side temperature rise of fibrous insulation. The results indicated that more efforts should be devoted to control the scatters in thermal loads and constituent properties to improve the reliability. The thermal reliability of fibrous insulation was predicted using the standard Monte-Carlo simulation technique and the interference analysis between the strength and load distributions, and agreement between the two was excellent. The results provide valuable information on a more rigorous design of fibrous insulation, thereby avoiding the usual, overly conservative, conventional deterministic safety factor approaches.

Acknowledgements

This work was supported by the National High Technology 863 Projects Foundation of China (No. 2006AA705317). The authors also gratefully acknowledge the financial support of the Center for Composite Materials and Structures of HIT in China.

References

[1] A.A. Mittenbergs, The materials problem in structural reliability, AIAA1966-2521, pp. 148–158.
[2] T.W. Clyne, I.O. Golosnoy, J.C. Tan, A.E. Markaki, Porous materials for thermal management under extreme conditions, Philosophical Transactions of the Royal Society A 364 (2006) 125–146.
[3] W.D. Goodrich, S.M. Derry, R.J. Maraia, Effects of aerodynamic heating and TPS thermal performance uncertainties on the Shuttle Orbiter, AIAA 79-1042, pp. 1–9.
[4] J.W. Haney, Orbiter entry heating lessons learned from development flight test program, NASA CP-2283, Part 2, March 8–10, 1983, pp. 719–752.
[5] M. Kamiński, Monte-Carlo simulation of effective conductivity for fiber composites, Int. Comm. Heat Mass Transfer 26 (6) (1999) 791–800.
[6] T. Nakamura, K. Fujii, Probabilistic transient thermal analysis of an atmospheric reentry vehicle structure, Aerospace Science and Technology 10 (2006) 346–354.
[7] S.L. Smith, G.B. Spear, M.D. Cornwell, Statistical Monte Carlo prediction for thermal reliability, AIAA94-3183, pp. 1–9.
[8] D. Xiu, G.E. Karniadakis, A new stochastic approach to transient heat conduction modeling with uncertainty, Int. J. Heat Mass Transfer 46 (2003) 4681–4693.
[9] M. Kamiński, T.D. Hien, Stochastic finite element modeling of transient heat transfer in layered composites, Int. Comm. Heat Mass Transfer 26 (6) (1999) 801–810.
[10] B.M. Nicolai, J.D. Baerdemaeker, Computation of heat conduction in materials with random variable thermophysical properties, International Journal for Numerical Methods in Engineering 36 (1993) 523–536.
[11] E.M. Sparrow, R.D. Cess, Radiation Heat Transfer, augmented ed., McGraw-Hill, New York, 1978.
[12] M.F. Modest, Radiative Heat Transfer, McGraw-Hill, New York, 1993.
[13] W.W. Yuen, G. Cunnington, Heat transfer characteristics of high porosity fibrous insulation materials (analysis of radiative heat transfer using the zonal-GEF method), AIAA 2005-192, pp. 1–12.
[14] K. Daryabeigi, Heat transfer in high-temperature fibrous insulation, AIAA Paper 2002-3332, pp. 1–15.
[15] J. Marschall, J. Maddren, J. Parks, Internal radiation transport and effective thermal conductivity of fibrous ceramic insulations, AIAA 2001-2822, pp. 1–15.
[16] R.K. Bhattacharyya, Heat transfer model for fibrous insulations, in: D.L. McElroy, R.P. Tye (Eds.), Thermal Insulation Performance, ASTM STP 718, American Society for Testing and Materials, Philadelphia, PA, 1980, pp. 272–286.
[17] L. Lees, C.Y. Liu, Kinetic theory description of conductive heat transfer from a fine wire, The Physics of Fluids 5 (10) (1962) 1137–1148.
[18] C.Y. Liu, L. Lees, Kinetic Theory Description of Plane Compressible Coquette Flow, Advances in Applied Mechanics, Academic Press, New York, 1961.
[19] E.H. Kennard, Kinetic Theory of Gases, McGraw-Hill Book Company, 1938.
[20] K. Daryabeigi, Thermal analysis and design of multi-layer insulation for re-entry aerodynamic heating, AIAA Paper 2001-2834, pp. 1–9.
[21] B.M. Zhang, S.Y. Zhao, X.D. He, Experimental and theoretical studies on high-temperature thermal properties of fibrous insulation, Journal of Quantitative Spectroscopy & Radiative Transfer 109 (2008) 1309–1324.
[22] M.L. Blosser, Advanced metallic thermal protection systems for reusable launch vehicles, Ph.D. dissertation, University of Virginia, 2000.
[23] R.R. Pettyjohn, Thermal conductivity measurements on the fibrous insulation material, in: Thermal Conductivity Proceedings of the Seventh Conference, 1967.
[24] D.J. Rasky, P. Kolodziej, M.E. Newfield, B. Laub, Y.K. Chen, Assessing factors of safety, margins of safety, and reliability of thermal protection systems, AIAA2003-4043, pp. 1–8.
[25] B.M. Ayyub, R.H. McCuen, Probability, Statistics and Reliability for Engineers, CRC Press, 1997.